Supporting Information

Hotspots on Action: Near-infrared Light Mediated Photo Electrochemical Oxygen Evolution on High Index Facet Plasmonic Gold Nano Architectures.

*Sanjeevan Rajagopal[1], Suresh Thangudu[1], June-Yen Feng[1], Pavithra Sriam[2], Ta-Jen Yen[2], and Kuo Chu Hwang[1]**

1. *Department of Chemistry, National Tsing Hua University, Hsinchu 30013, Taiwan, R.O.C.*

2. *Department of Materials Science and Engineering, National Tsing Hua University, Hsinchu, 30013, Taiwan, R.O.C.*

*E-mail: kchwang@mx.nthu.edu.tw

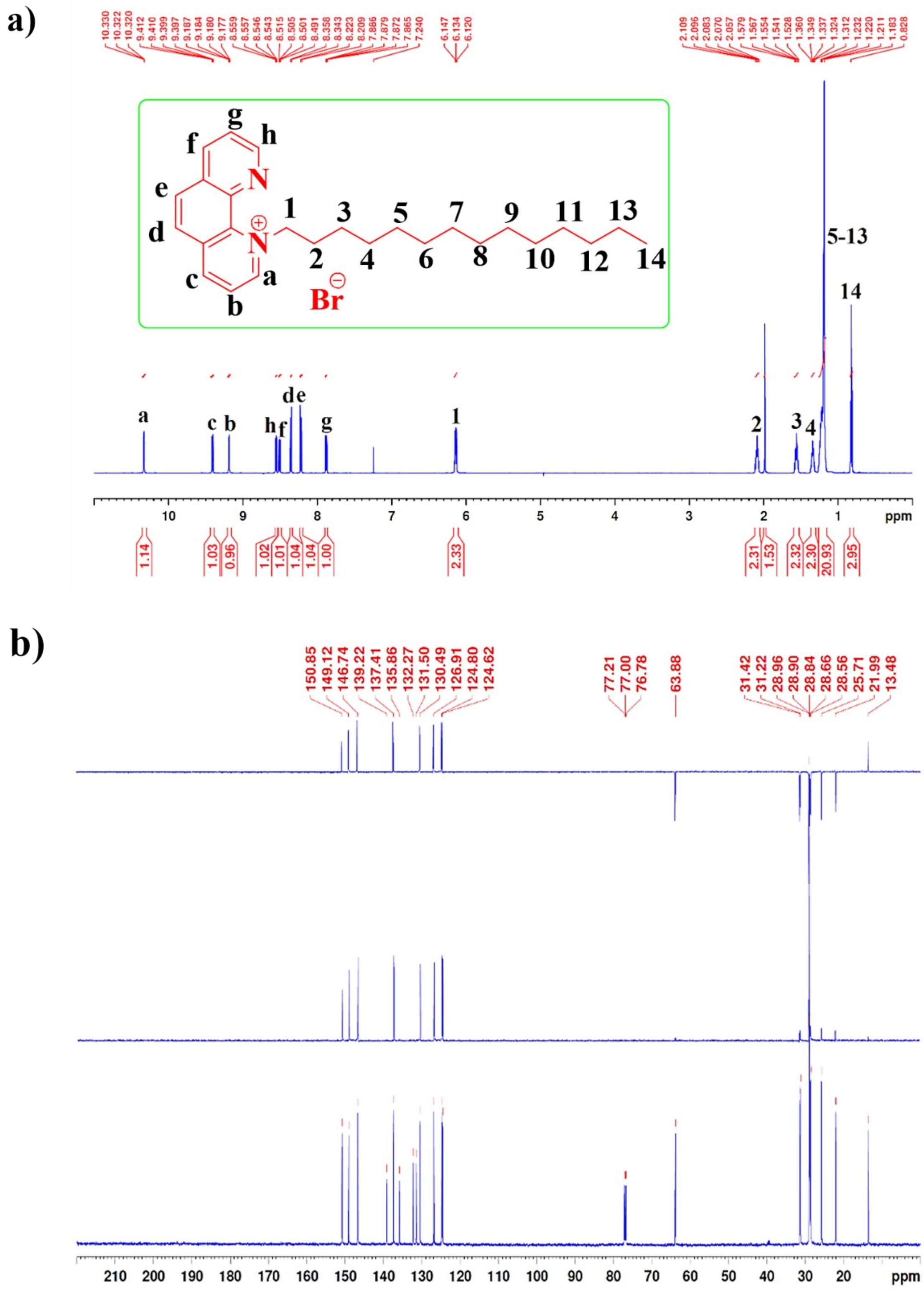

Figure S1. (**a**) ^{1}H-NMR and (**b**) ^{13}C-NMR for 1-tetradecyl-1, 10-phenanthroline-1-ium bromide surfactant dissolved in D-chloroform solvent.

(1-tetradecyl-1, 10-phenanthrolin-1-ium bromide)

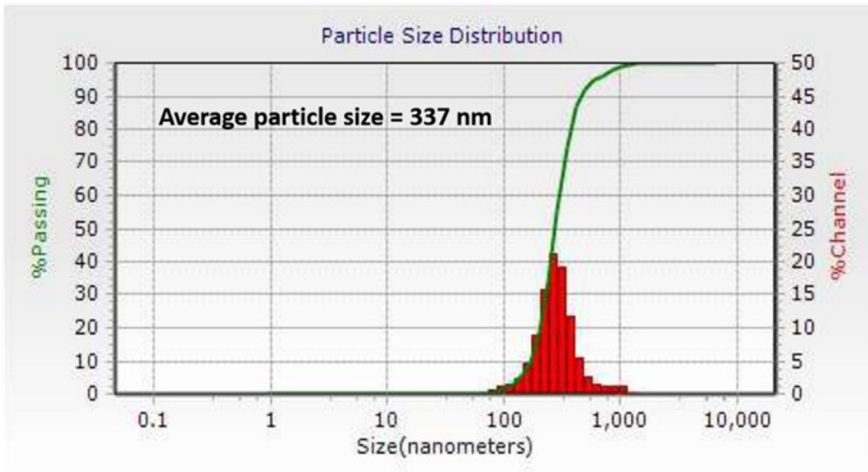

Figure S2. Dynamic light scattering analysis spectra of Au 12 tips aqueous solution (DLS, model W3180, Microtrac).

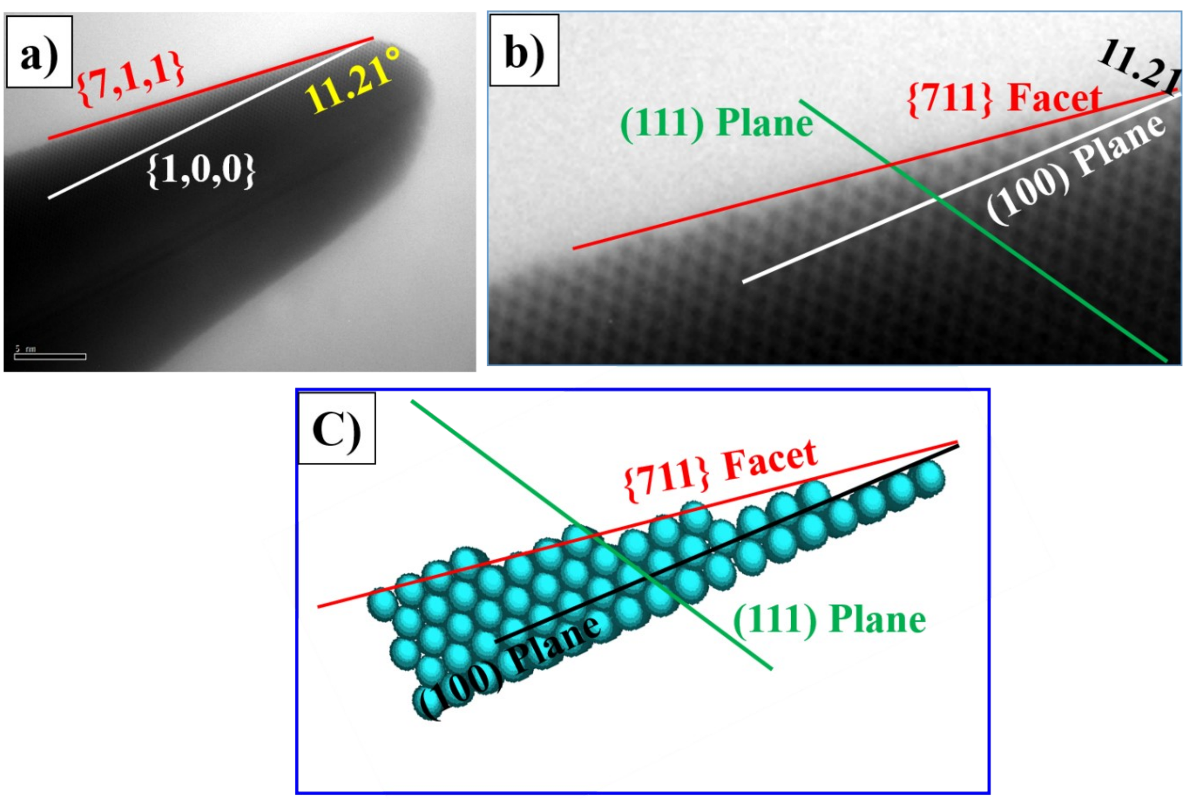

Figure S3. (a) TEM image of one of the sharp tips of Au 12 tips nanostars. (b) HRTEM image, (**c**) the atomic model of the {711} planes projected along the [-1, 1, 1] and [-1, 1, 0] zone axis.

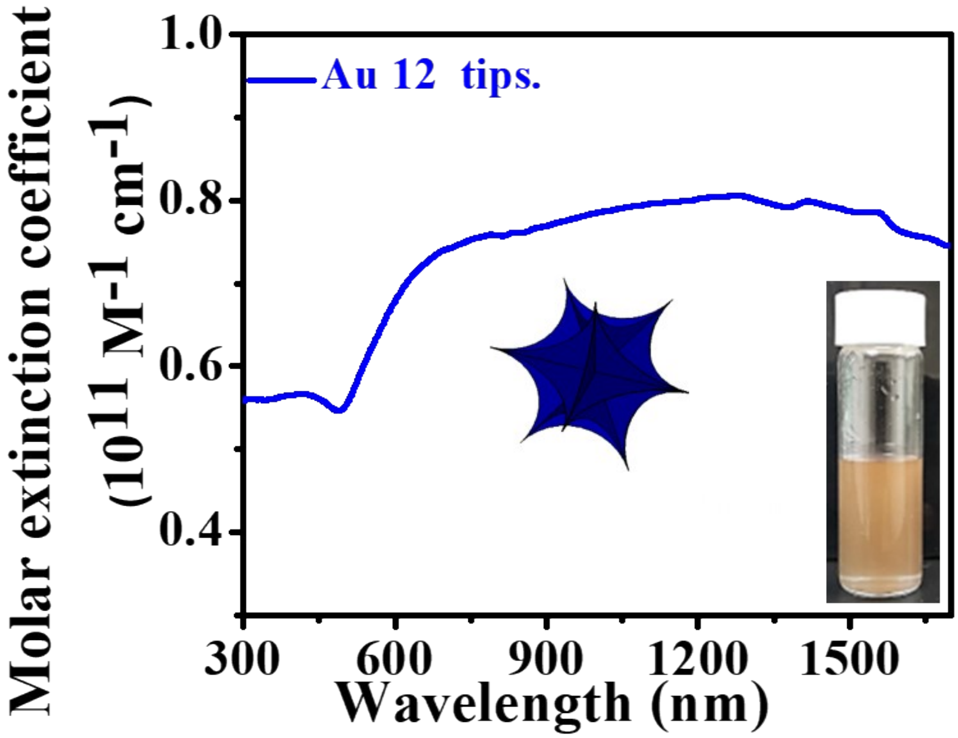

Figure S4. Molar extinction coefficients of Au 12 tips nanostars as a function of wavelengths (The inset shows the optical image of Au 12 tips nanostars-containing aqueous dispersion).

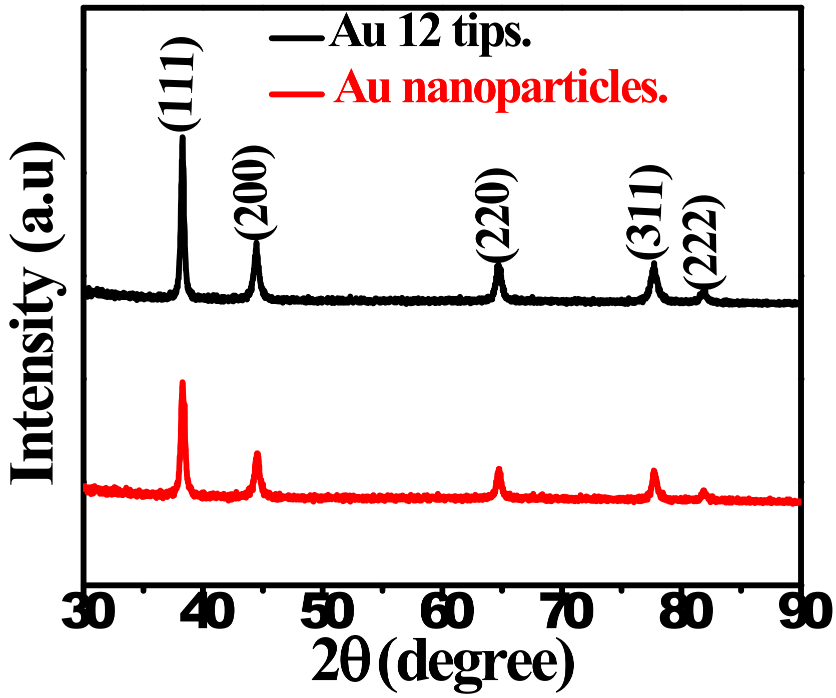

Figure S5. XRD pattern for Au 12 tips nanostars and Au nanoparticles.

(a)

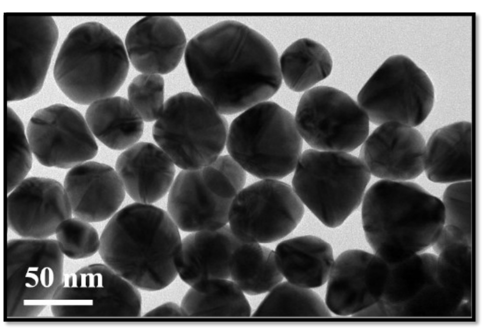

(b)

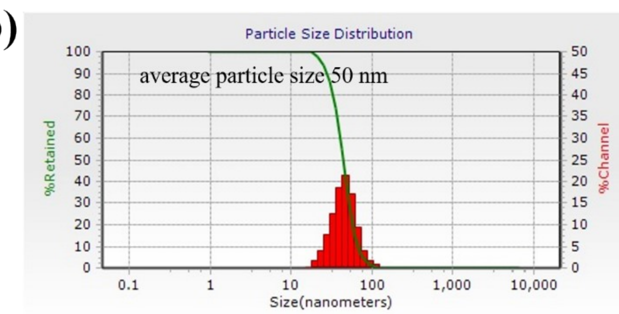

Figure S6. (a) TEM image and (b) DLS spectra of Au nanoparticles.

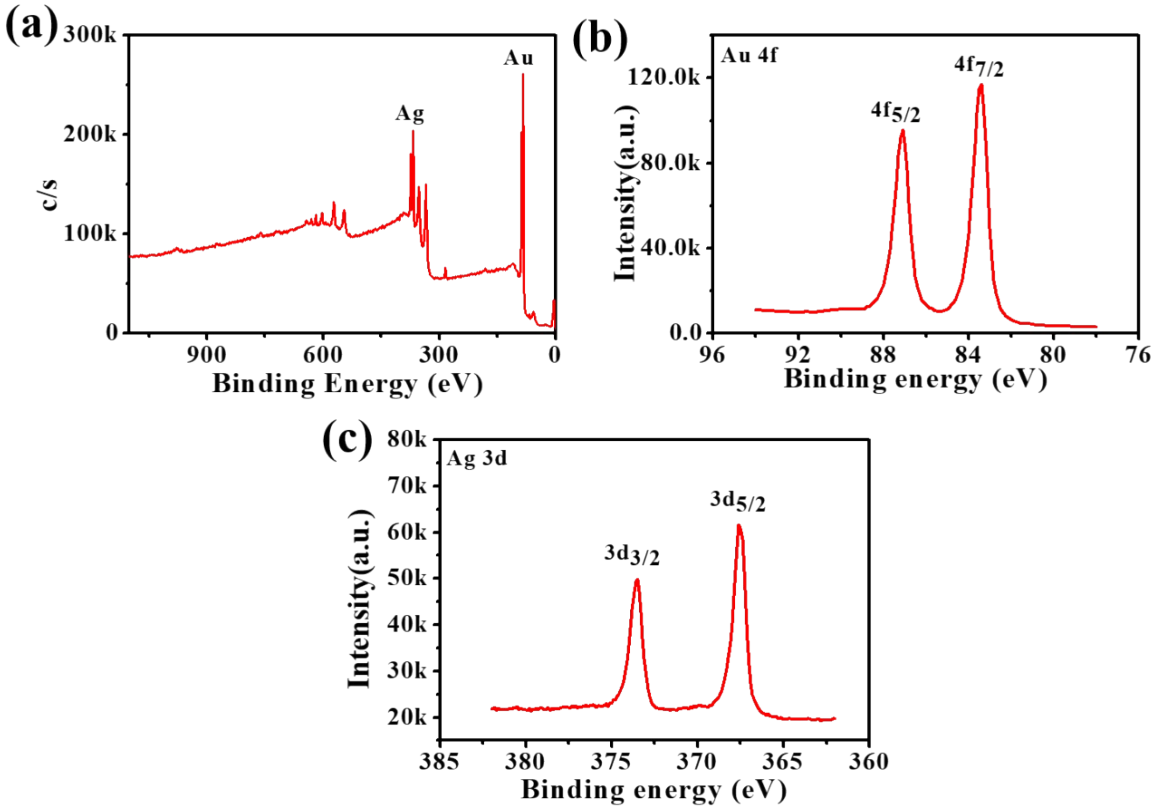

Figure S7. XPS spectra of Au 12 tips nanostars, (a) survey scan (b) high-resolution of Au 4f, and (c) high-resolution of Ag 3d.

(a)

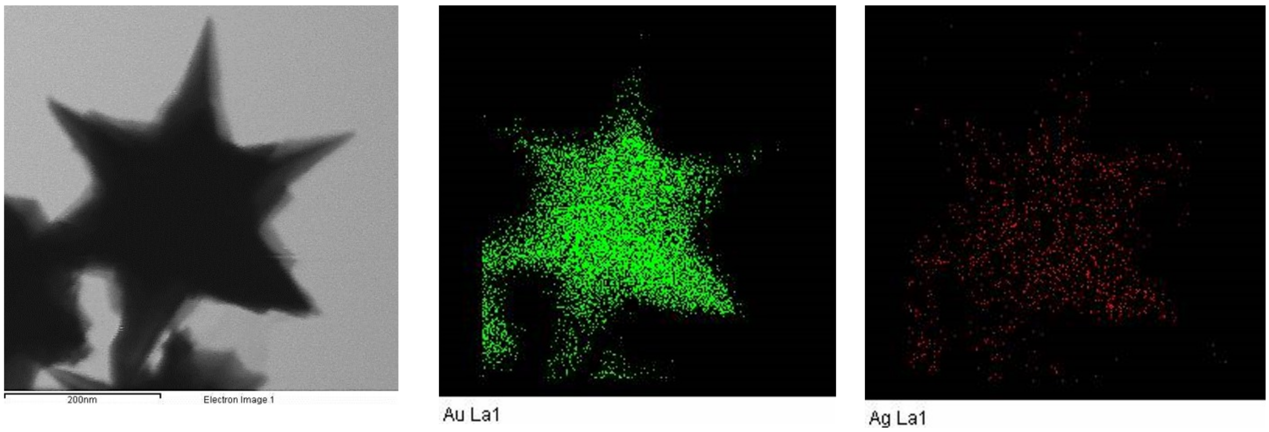

(b)

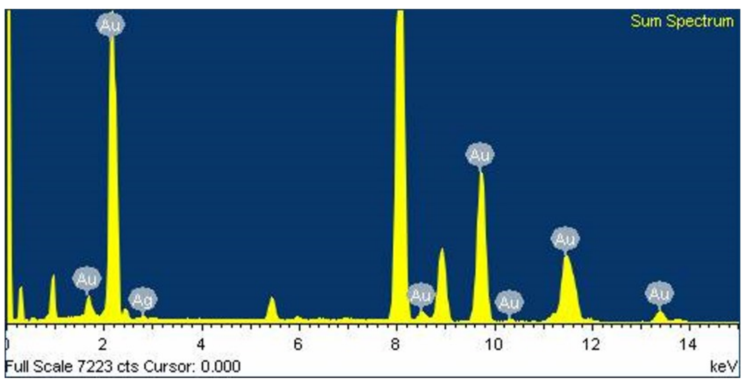

Element	Weight%	Atomic%
Ag L	0.37	0.67
Au L	99.63	99.33

Figure S8. (a) EDX elemental mapping for Au 12 tips nanostars, (b) the corresponding EDX elemental spectrum and atomic percentage.

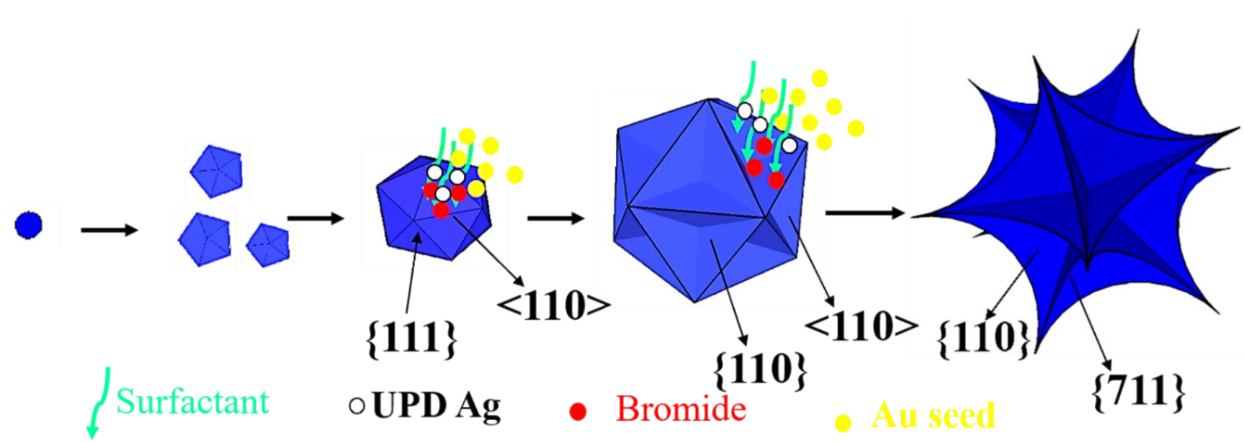

Figure S9. Schematic illustration of the formation and growth mechanism of Au 12 tips nanostars.

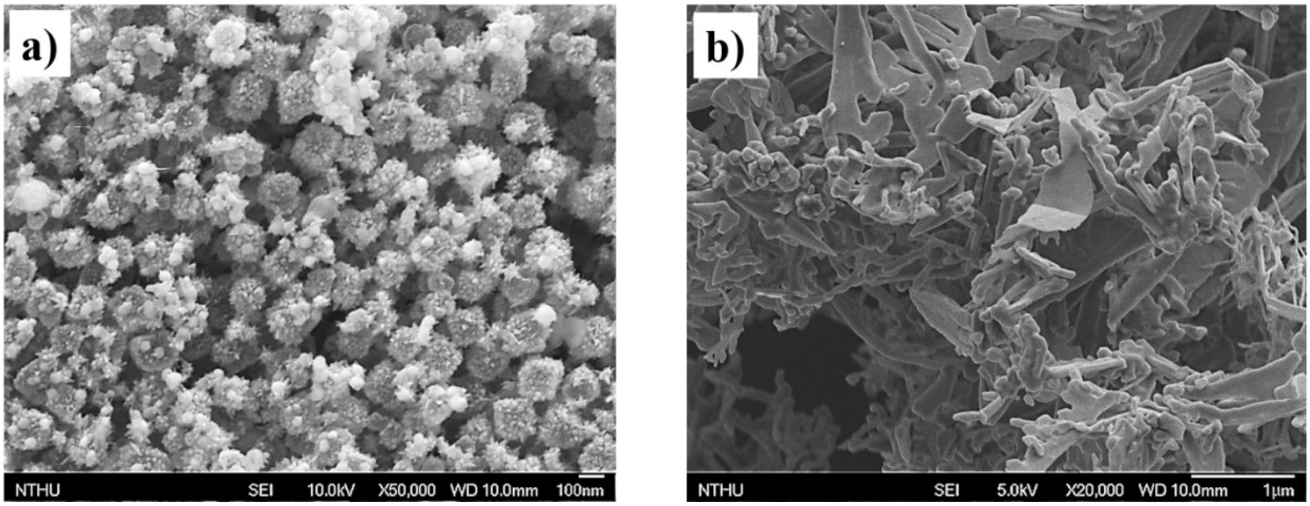

Figure S10. SEM images (a) without TDPB surfactant and (b) without $AgNO_3$.

Time (minutes)	Intensity ratio of I(111)/I(200)
60	3.78
45	3.73
30	3.65
15	3.54
10	3.17
5	2.70
2	1.95

Figure S11. XRD peak intensity ratio (111) / (200) during the formation of Au 12 tips nanostars.

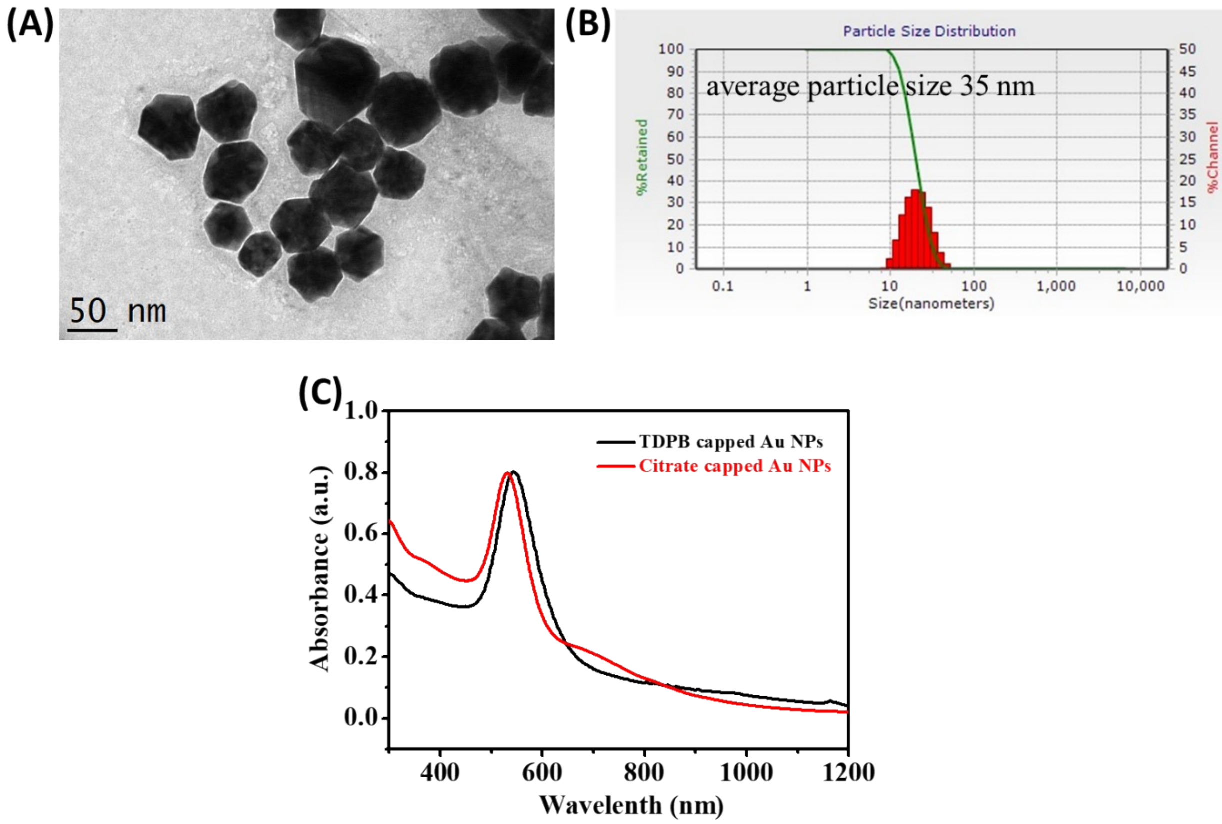

Figure S12. TDPB coated Au NPs. (A) TEM image of Au NPs, (B) DLS size distribution spectra, (C) absorption spectra of NPs. (D) LSV curves corresponding to the photoelectrochemical OER on TDPB-capped Au NPs under dark, 532 nm and 915 nm laser irradiation conditions.

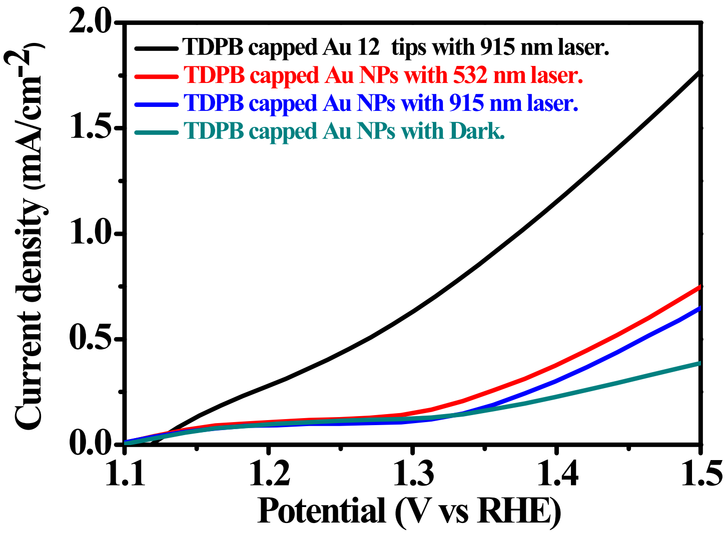

Figure S13. LSV curves corresponding to the photoelectrochemical OER on TDPB-capped Au NPs and TDPB-capped Au 12 tips-electrodes under dark and light conditions, respectively.

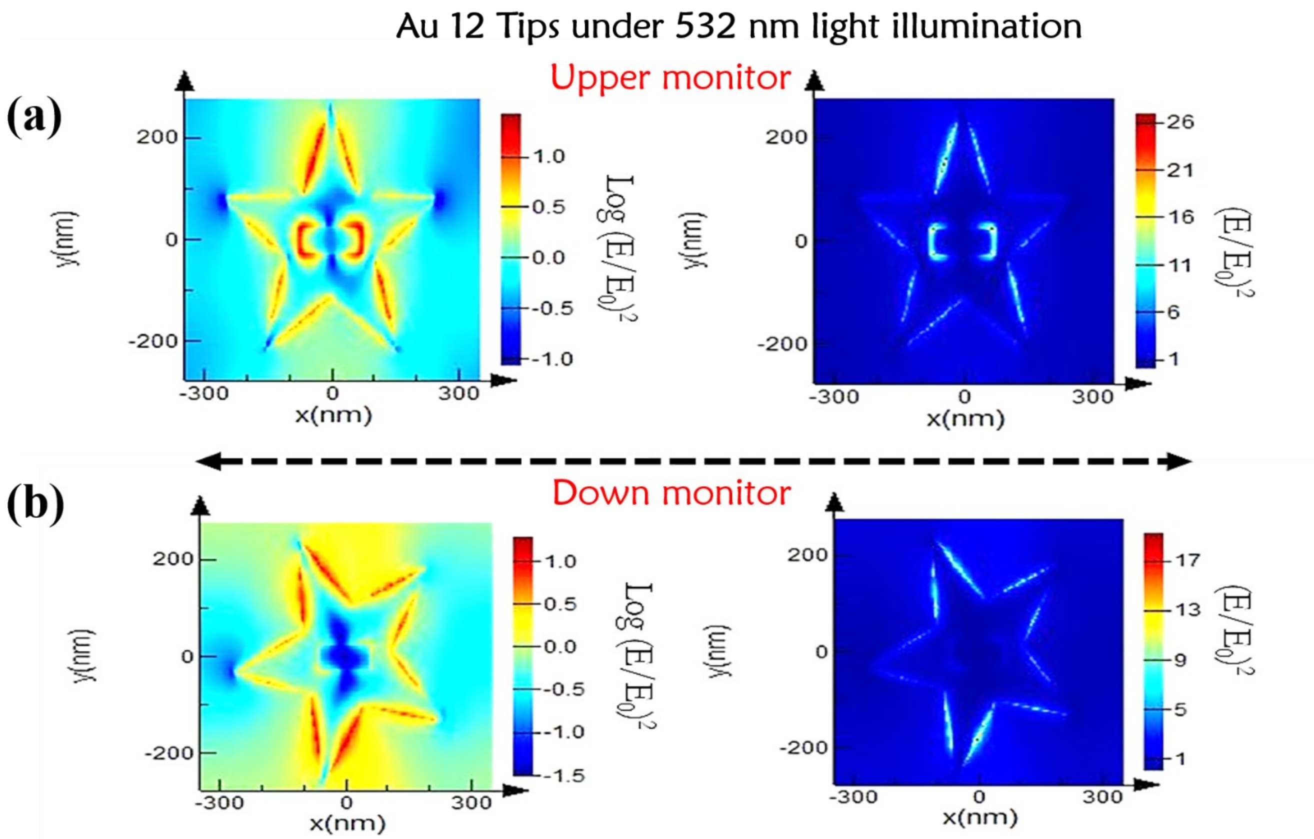

Figure S14. FDTD calculated the local electric field Au 12 tips under 532 nm (a) upper monitor and (b) down the monitor.

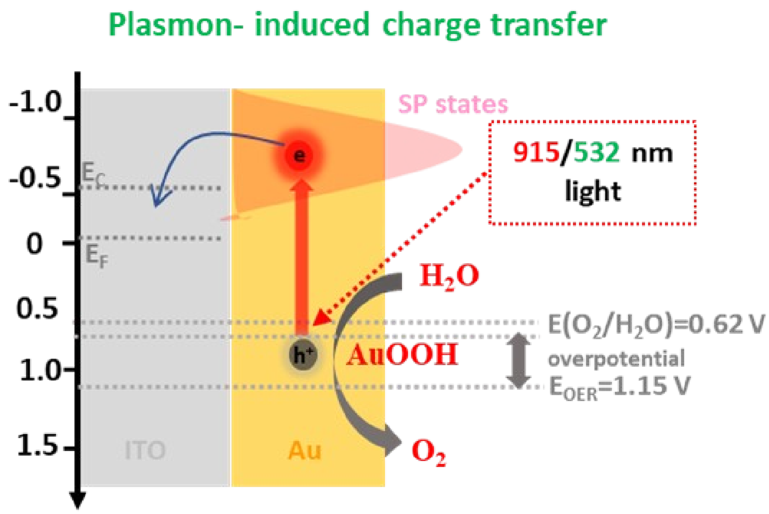

Figure S15. Schematic illustration of photocatalytic mechanism of OER on Au 12 tips-electrode.

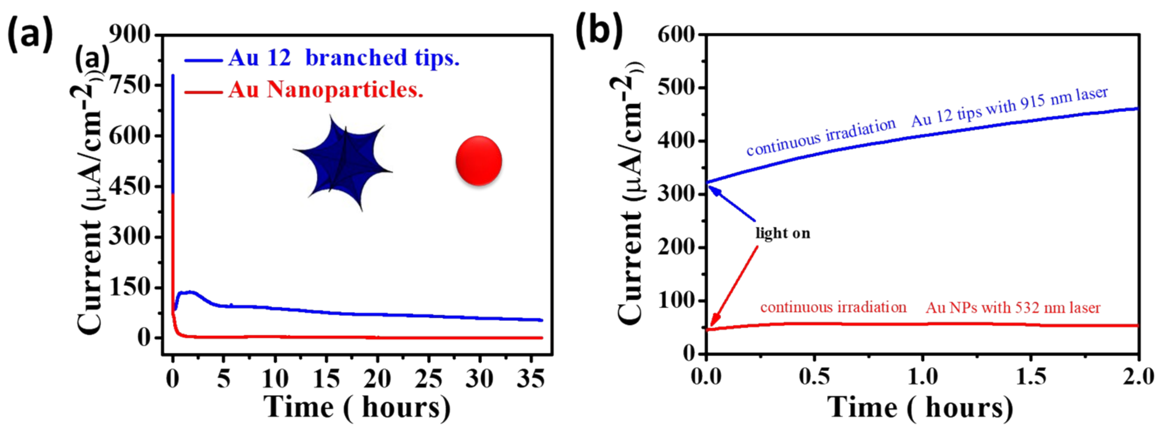

Figure S16. (a) Stability test performed on Au 12 tips- and Au NPs-electrodes in the dark. (b) Chrono potentiometric curves of Au 12 tips and Au NPs electrodes under laser irradiation, respectively. The externally applied voltage is 0.6 V vs. RHE.

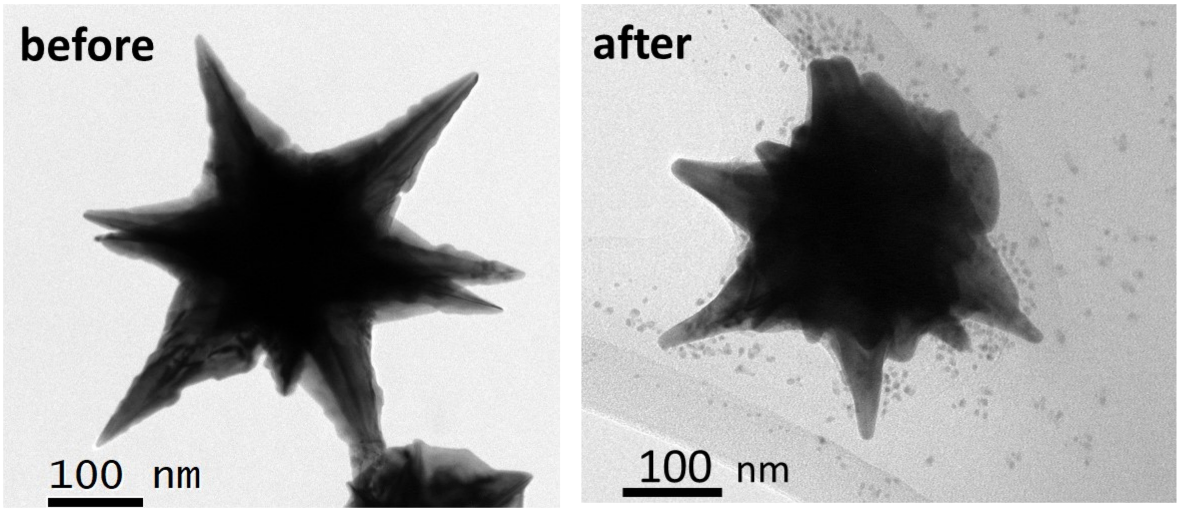

Figure S17. TEM images for Au 12 tips nanostars before catalytic performance and after catalytic performance.

Table S1 High index facets of Au 12 tips nanostars with different projection angles.

Angle with {100}	**55°**	**35°**	**25°**	**19°**	**15°**	**13°**	**11°**
{h11}	**{111}**	**{211}**	**{311}**	**{411}**	**{511}**	**{611}**	**{711}**

Table S2 Summary of recent developments regarding oxygen evolution reaction (OER) using plasmonic photoelectrodes.

Plasmonic Photoelectrode	**Electrolyte**	**Light Source**	**Photocurrent density (mA/cm^{-2})**	**Ref.**
Au@TiO_2 nanotube arrays	1.0 M KOH	150 W Xenon lamp cutoff filter >415 nm	0.1 mA/cm^{-2} vs. RHE	S1
Au@$BiVO_4$	0.1 M PBS	300 W Xenon lamp AM 1.5 Filter 100 mW cm^{-2}	0.6 mA/cm^{-2} vs. RHE	S2
Au@WO_3	0.5 M Na_2SO_4	150 W Xenon lamp AM 1.5 Filter 100 mW cm^{-2}	0.8 mA/cm^{-2} vs Ag/AgCl	S3

SiO2 @Ag/$BiVO_4$	0.5 M KH_2PO_4	300 W Xenon lamp AM 1.5 Filter 100 mW cm^{-2}	5.0 mA/cm^{-2} vs. Ag/AgCl	S4
Au NPs@$Ti_3C_2T_x$	1.0 M KOH	525 nm laser 100 mW cm^{-2}	8.0 mA/cm^{-2} vs. RHE	S5
$BiVO_4$ /Co(OH)x-Ag	0.5 M Na_2SO_4	300 W Xenon lamp AM 1.5 Filter 100 mW cm^{-2}	4.0 mA/cm^{-2} vs. RHE	S6
Ag@$BiVO_4$	0.5 M Na_2SO_4	300 W Xenon lamp AM 1.5 Filter 100 mW cm^{-2}	1.7 mA/cm^{-2} vs. RHE	S7
Au NRs	1.0 M KOH	808 nm laser, 200 mW cm^{-2}	0.5 mA/cm^{-2} vs. RHE	S8
Au 12 tips-electrode	**0.1 M KOH**	**915 nm laser 300 mW cm^{-2}**	**1.8 mA/cm^{-2} vs. RHE**	**Current work**

TDPB surfactant crystal structure information

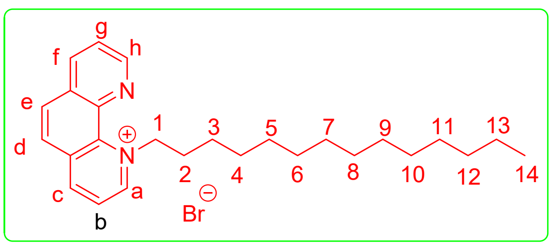

Apple white powder; ^{1}**H NMR** (600 MHz, $CDCl_3$): δ 10.33 (s, 1 H), 9.40 (d, J= 12.0 Hz, 1 H), 9.18 (s, 1 H), 8.54 (d, J= 6.0 Hz, 1 H), 8.50 (d, J= 6.0 Hz, 1H), 8.34 (d, J= 6.0 Hz, 1H), 8.21 (d, J= 12.0 Hz, 1H), 7.87 (d, J= 12.0 Hz, 1H), 6.13 (t, J= 6.0 Hz, 2H), 2.09-2.06 (m, 2H), 1.56 -1.54 (m, 2H), 1.34-1.32 (m, 2H), 1.24 – 1.18 (m, 20 H), 0.81 (t, J = 6.0 Hz, 3 H).

^{13}**C NMR** (150 MHz, $CDCl_3$): 150.8, 149.1, 146.7, 139.2, 137.4, 135.8, 132.2, 131.5, 130.4, 126.9, 124.8, 124.6, 63.8, 31.4, 31.2, 28.9, 28.9, 28.8, 28.6, 28.5, 25.7, 21.9, and 13.4.

ORTEP diagram of the solid product surfactant

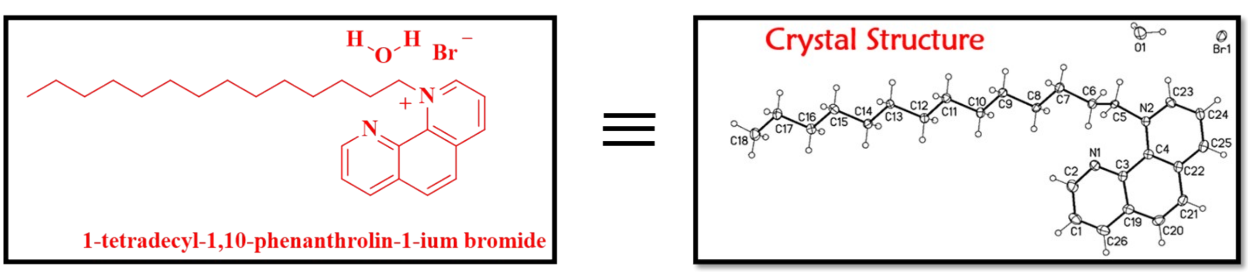

Crystal data and structure refinement for mo_160548LT_0m.

Identification code	mo_160548LT_0m	
Empirical formula	C26 H39 Br N2 O	
Formula weight	475.50	
Temperature	100(2) K	
Wavelength	0.71073 Å	
Crystal system	Triclinic	
Space group	P -1	
Unit cell dimensions	a = 8.6383(17) Å	a= 102.453(5)°.
	b = 11.793(2) Å	b= 91.642(5)°.
	c = 25.970(6) Å	g = 108.802(5)°.
Volume	2431.8(9) $Å^3$	
Z	4	
Density (calculated)	1.299 Mg/m^3	
Absorption coefficient	1.710 mm^{-1}	
F(000)	1008	
Crystal size	0.15 x 0.10 x 0.10 mm^3	
Theta range for data collection	0.808 to 26.532°.	
Index ranges	-10<=h<=9, -14<=k<=14, -31<=l<=32	
Reflections collected	37218	
Independent reflections	10037 [R(int) = 0.0679]	
Completeness to theta = 25.242°	100.0 %	
Absorption correction	Semi-empirical from equivalents	
Max. and min. transmission	0.9485 and 0.8634	
Refinement method	Full-matrix least-squares on F^2	
Data / restraints / parameters	10037 / 0 / 543	
Goodness-of-fit on F^2	0.993	
Final R indices [I>2sigma(I)]	R1 = 0.0396, wR2 = 0.0845	
R indices (all data)	R1 = 0.0759, wR2 = 0.1012	
Extinction coefficient	n/a	
Largest diff. peak and hole	0.438 and -0.439 e.$Å^{-3}$	

Supporting reference:

S1. S. Y. Moon, H.C. Song. E. H. Gwag. I.I. Nedrygailov, C Lee, J. J. Kim, W, H, Doh, and J, Y, Park. *Nanoscale*, 2018, **10,** 22180–22188.

S2. T. G. U. Ghobadi, A. Ghobadi, M. C. Soydan, M. B. Vishlagh, S. Kaya, F. Karadas, E. Ozbay *ChemSusChem*, 2020, **13,** 2577 –2588.

S3. Y. Liu, Y. S. Chang, Y. J. Hsu, B. J. Hwang, and C. H. Hsueh, *Electrochim. Acta*, 2019, **321,**134674

S4. S. Caliskan, J. K. Kim, G. S. Han, F. Qin, I.. S. Cho, H. S. Han, and J. K. Lee, *ACS Appl. Energy Mater.,* 2020, **3,** 11886−11892.

S5. J. Wang, X. Wei, X. Wang, W. Song, W. Zhong, M. Wang, J. Ju, and Y. Tang, *Inorg. Chem*., 2021, **60,** 5890−5897.

S6. X. Ning, D. Yin, Y. Fan, Q. Zhang, P. Du, D. Zhang, J. Chen, and X. Lu, *Adv. Energy Mater.,* 2021, **11,** 2100405.

S7. S. Y. Jeong, H. M. Shin, Y. R. Jo, Y. J. Kim, S. Kim, W. J. Lee, G. J. Lee, J. Song, B. J. Moon, S. Seo, H. An, S. H. Lee, Y. M. Song, B.J. Kim, M. H. Yoon, and S. Lee, *J. Phys. Chem. C*, 2018, **122,** 7088−7093.

S8. W. Zhang, S. Wang, S. A. Yang, X. H. Xia, and Y. G. Zhou, *Nanoscale*, 2020, **12,** 17290–17297.